

Plasma proteomics identify biomarkers and undulating changes of brain aging

Received: 4 March 2024

Accepted: 17 October 2024

Published online: 09 December 2024

 Check for updates

Wei-Shi Liu¹, Jia You², Shi-Dong Chen¹, Yi Zhang¹, Jian-Feng Feng^{2,3},
Yu-Ming Xu^{4,5}✉, Jin-Tai Yu¹✉ & Wei Cheng^{1,2,3}✉

Proteomics enables the characterization of brain aging biomarkers and discernment of changes during brain aging. We leveraged multimodal brain imaging data from 10,949 healthy adults to estimate brain age gap (BAG), an indicator of brain aging. Proteome-wide association analysis across 4,696 participants of 2,922 proteins identified 13 significantly associated with BAG, implicating stress, regeneration and inflammation. Brevican (BCAN) ($\beta = -0.838$, $P = 2.63 \times 10^{-10}$) and growth differentiation factor 15 ($\beta = 0.825$, $P = 3.48 \times 10^{-11}$) showed the most significant, and multiple, associations with dementia, stroke and movement functions. Dysregulation of BCAN affected multiple cortical and subcortical structures. Mendelian randomization supported the causal association between BCAN and BAG. We revealed undulating changes in the plasma proteome across brain aging, and profiled brain age-related change peaks at 57, 70 and 78 years, implicating distinct biological pathways during brain aging. Our findings revealed the plasma proteomic landscape of brain aging and pinpointed biomarkers for brain disorders.

The levels of aging populations are on the rise globally, and it is predicted that, by 2050, the number of individuals aged 65 years and above will exceed 1.5 billion¹. Aging is associated with a decline in homeostasis and resilience of the brain², which contribute to both functional deterioration and structural abnormalities². Aging and neurodegenerative disorders are closely correlated and highly overlapped^{3,4}; the prevalence of neurodegenerative disorders significantly increases with aging⁴. However, effective therapies for neurodegenerative disorders are limited⁴. Because neurodegenerative disorders and cerebrovascular diseases are common manifestations of brain aging^{5,6}, the early identification and intervention of brain aging is a promising strategy in the prevention of neurodegenerative disorders. Previous studies have pinpointed putative markers for brain aging, including imaging traits^{7,8} and histologic features^{9,10}. However, because these approaches provide limited molecular insight into brain aging, it is necessary to discover new biomarkers for brain aging.

To stratify those at different risk or clinical stages of brain disorders, brain age is proposed to estimate brain health status¹¹. Utilizing multimodal brain magnetic resonance imaging (MRI) and machine learning models, BAG—the deviation between predicted brain age and chronological age—can be generated and used as a potential indicator of brain health^{11,12}. Previous studies have demonstrated the associations between BAG and multiple neuropsychiatric disorders, including Alzheimer's disease (AD)^{13,14}, Parkinson's disease (PD)¹⁵, depression¹⁶, schizophrenia¹⁷ and stroke¹⁸. Omics-based techniques have enabled the discovery of biomarkers of brain aging. One previous study identified genomic regions associated with BAG¹⁹. Proteins are the direct regulators of biological pathways, which provide direct evidence for aging²⁰. The use of proteomics has discovered multiple plasma proteins that change with chronological age^{21,22}. Blood serves as a mediator between the brain and periphery, with changes in plasma protein abundance reflecting alterations in the

¹Department of Neurology and National Center for Neurological diseases, Huashan Hospital, State Key Laboratory of Medical Neurobiology and MOE Frontiers Center for Brain Science, Shanghai Medical College, Fudan University, Shanghai, China. ²Institute of Science and Technology for Brain-inspired Intelligence, Fudan University, Shanghai, China. ³Key Laboratory of Computational Neuroscience and Brain-Inspired Intelligence, Fudan University, Ministry of Education, Shanghai, China. ⁴Department of Neurology, The First Affiliated Hospital of Zhengzhou University, Zhengzhou, China. ⁵NHC Key Laboratory of Prevention and Treatment of Cerebrovascular Diseases, The First Affiliated Hospital of Zhengzhou University, Zhengzhou University, Zhengzhou, China. ✉e-mail: xuyuming@zzu.edu.cn; jintai_yu@fudan.edu.cn; wcheng@fudan.edu.cn

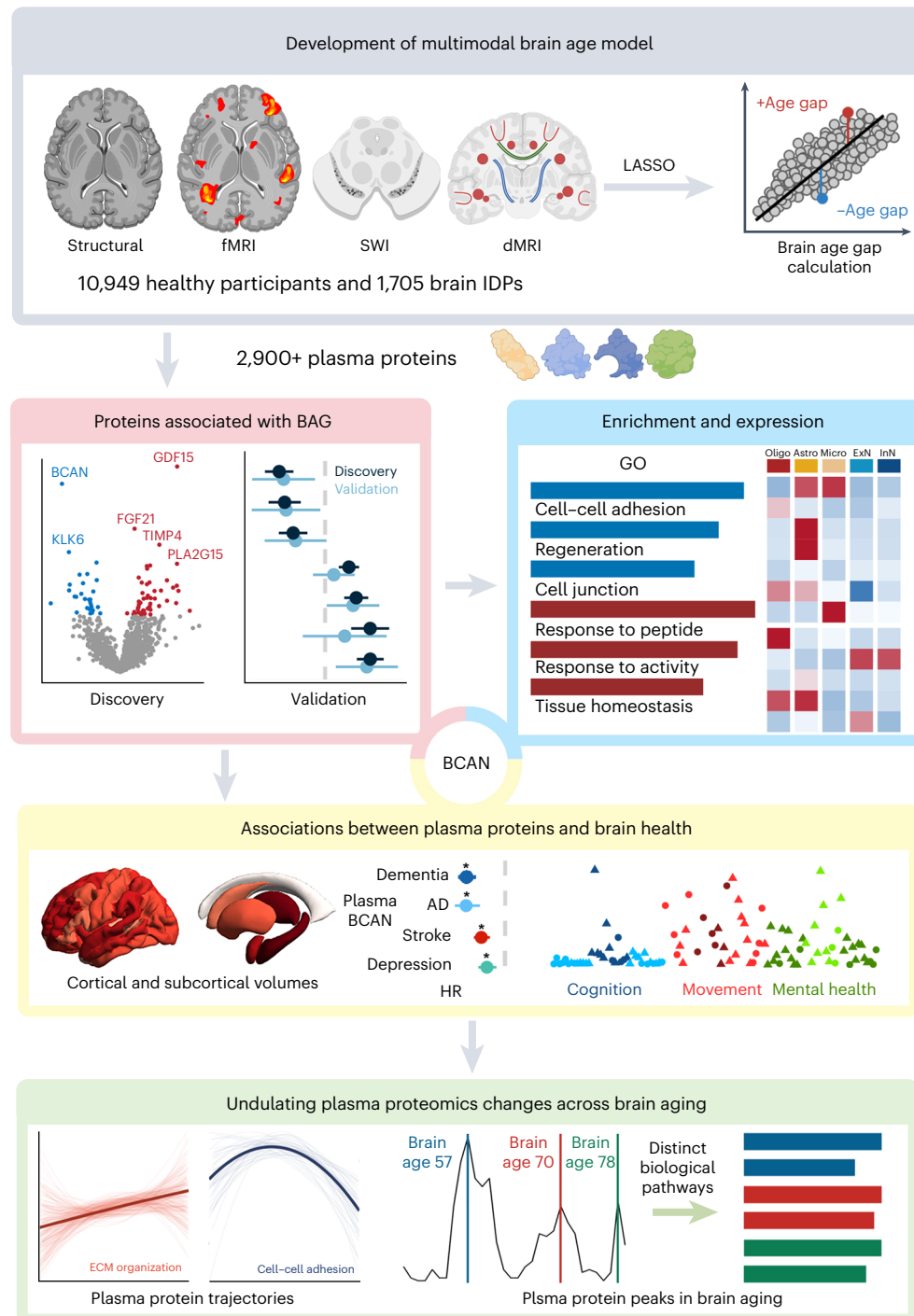


Fig. 1 | Graphical abstract. Top, the present study used multimodal brain imaging data, including 1,705 brain IDPs of 10,949 healthy participants, to estimate brain age by LASSO; BAG, the deviation of brain age from chronological age, was then calculated. Middle, we used the plasma proteomics data of >2,900 proteins to conduct protein-wide association analysis of BAG, and validated the results above at the repeat imaging visit. Next, biological functions and expression levels in different cell types within the brain were further profiled. Moreover, the associations of BAG proteins with brain function, brain disorders

and brain structures were further tested. These findings suggested BCAN as a putative biomarker for brain aging. Bottom, we characterized undulating changes in plasma proteins during brain aging and identified both linear and nonlinear patterns. In addition, we identified essential time periods during brain aging; proteins at these time periods had distinct biological pathways. ECM, extracellular matrix; ExN, excitatory neuron; fMRI, functional MRI; InN, inhibitory neuron; SWI, susceptibility-weighted imaging.

brain associated with neuropsychiatric disorders, due to the bidirectional communication between the central nervous system and peripheral circulation^{23,24}. In addition, measurements based on blood are minimally invasive and easily accessible, and previous studies have revealed peripheral proteins associated with aging or neurodegenerative disorders^{20,25}. However, little is known about how plasma proteomes change with brain

aging. Investigating the dynamics of plasma proteome during brain aging is essential for revealing the molecular mechanisms associated with brain disorders. Bridging this knowledge gap also provides potential for the early identification and intervention of neurodegenerative disorders.

In this study, we integrated multimodal brain imaging data and plasma proteome data from UK Biobank to investigate changes in

peripheral proteomes across brain aging. Initially, we developed a multimodal brain age model and identified those plasma proteins associated with BAG. Next, we characterized their biological functions and cellular expressions in the brain, and discovered the clinical implications for brain health. Finally, we profiled changes in the proteome across brain aging in a cross-sectional cohort, and identified three important plasma proteomic peaks of brain aging (Fig. 1).

Results

Development of the multimodal brain age model

For calculation of multimodal brain age (Supplementary Fig. 1), we screened brain imaging-derived phenotype (IDP) data, selecting 1,705 IDPs as input for brain age calculation (Supplementary Table 1). Following exclusion of participants with neuropsychiatric and other disorders (for example, hypertension, atherosclerosis and others; Supplementary Table 2) and those with plasma proteomics data, 10,949 participants remained. These participants were divided into a training and a testing set, using the least absolute shrinkage and selection operator (LASSO) regression approach to develop brain age (Supplementary Table 3). Finally, 864 brain IDPs were included and we obtained brain age estimates with a mean absolute error of 2.76 in all individuals in the testing set; model performance was found to be better among females than males (Fig. 2a).

Proteome-wide association of BAG

To identify those proteins associated with brain aging, we screened participants with both multimodal brain imaging data and plasma proteomics data ($n = 4,696$), predicted brain age and then calculated BAG. Participants had a mean age of 63.16 years and comprised 53.6% females and 97.1% white ethnicities (Supplementary Table 4). Following Bonferroni correction (adjusted $P = 1.71 \times 10^{-5}$), 13 proteins significantly associated with BAG were identified, among which there were eight positive associations: growth differentiation factor 15 (GDF15), fibroblast (Fibro) growth factor 21 (FGF21), tissue inhibitors of matrix metalloproteinase 4 (TIMP4), lysosomal phospholipase A and acyltransferase (PLA2G15), glial fibrillary acidic protein (GFAP), adhesion G protein-coupled receptor G1 (ADGRG1), galectin-4 (LGAL4S), CHI3L1 chitinase 3-like protein 1 (CHI3L1); and five negative associations: BCAN, kallikrein-6 (KLK6), carcinoembryonic antigen-related cell adhesion molecule 16 (CEACAM16), WAP, Kazal, immunoglobulin, Kunitz and NTR domain-containing protein 1 (WFIKKN1) and ADAM22 disintegrin and metalloproteinase domain-containing protein 22 (ADAM22) (Fig. 2b and Supplementary Table 5). We also performed additional analyses for the repeat imaging visit to validate the above results. We found that six proteins were nominally associated with BAG ($P < 0.05$) and survived in validation analysis (Fig. 2c): LGALS4, ADGRG1, GDF15, BCAN, KLK6 and TIMP4 (Supplementary Table 6).

The biological functions of those proteins associated with BAG, following false discovery rate, correction were further profiled (Supplementary Table 7). Biological processes, including the tyrosine kinase signaling pathway, were the top pathways nominally enriched ($P < 0.05$) in proteins positively associated with BAG, indicating increasing age-related degradation and stress state in brain aging. Proteins negatively associated with BAG were mainly associated with cell–cell adhesion and neuron projection regeneration, implicating neuronal dysfunction as a major component of brain aging (Fig. 2d). Downregulated proteins were mainly located in synapses (Supplementary Table 7). In addition, it was noted that upregulated proteins were mainly enriched in cellular components such as extracellular matrix and lumen.

Expression-based analysis of proteins associated with BAG

The cellular expression levels of BAG protein-coding genes were profiled, leveraging peripheral blood mononuclear cell single-cell RNA sequencing data from both young and old individuals (Supplementary Table 8).

Although nine BAG protein-coding genes were detected (Supplementary Figs. 2 and 3), most of these were not highly expressed in peripheral blood except for ADGRG1 (Supplementary Fig. 4). We further leveraged human brain single-nucleus RNA sequencing (snRNA-seq) data (Supplementary Figs. 5 and 6). In addition to *FGF21*, 12 BAG protein-coding genes were detectable in 61,862 individual cells from 17 samples (Fig. 2e). *GFAP*, *CHI3L1* and *CEACAM16* were mainly expressed by astrocytes (Astro). *BCAN* was expressed mainly in oligodendrocyte (Oligo) progenitor cells (OPCs) and Astro, while *GDF15* and *WFIKKN1* were predominantly expressed in Fibro.

To test whether the expression levels of BAG protein-coding genes were altered in age-related neurodegenerative disorders, we obtained AD snRNA-seq data from 61,251 cells (Supplementary Figs. 7 and 8) and found that *BCAN* was downregulated in both OPCs and Astro in AD (Supplementary Fig. 9); in addition, the expression level of *CHI3L1* in Astro was upregulated (Supplementary Fig. 9). Overall, the data at transcription level supported the candidate roles of BAG proteins in brain aging and related disorders, particularly BCAN.

Associations between BAG proteins and brain structures

The associations between BAG proteins and brain structures were further profiled (Supplementary Table 9). Following Bonferroni correction (only the 13 significant proteins associated with BAG were considered here), both BCAN and KLK6 showed the most associations with cortical and subcortical structures, particularly cortical volume, cortical surface area and subcortical volume (Fig. 3a). Although there were few associations between plasma GFAP and cortical structures, it had the most associations with white matter tracts (Fig. 3a).

Brevican was significantly associated with volume and surface area of 47 and 61 cortical regions, respectively, and there were 43 and 64 significant associations between KLK6 and cortical volume and surface area, respectively. Most BAG proteins showed significant associations with frontal and temporal volumes (Fig. 3b), which demonstrated obvious atrophy in aging or neurodegenerative disorders². In addition, BCAN was associated with volume in 12 subcortical regions (Fig. 3c). The full results of these associations with brain structures are given in Supplementary Table 10. Overall, these findings highlight the intricate roles of BAG proteins in major brain regions in brain aging and age-related brain disorders, and further support the roles of candidate BAG proteins in brain aging.

Associations between BAG proteins and brain disorders

We further tested the associations between 13 BAG proteins and incident brain disorder risks (Fig. 4a). Following Bonferroni correction, BCAN was associated with lower risk of all-cause dementia (ACD; hazard ratio (HR) = 0.613, $P = 4.11 \times 10^{-11}$), AD (HR = 0.625, $P = 5.26 \times 10^{-6}$) and stroke (HR = 0.716, $P = 1.01 \times 10^{-6}$). WFIKKN1 was associated with lower risk of ACD (HR = 0.802, $P = 4.46 \times 10^{-4}$), stroke (HR = 0.799, $P = 1.15 \times 10^{-4}$), anxiety (HR = 0.823, $P = 7.28 \times 10^{-6}$) and depression (HR = 0.823, $P = 4.21 \times 10^{-5}$). GDF15 was significantly associated with higher risk of ACD (HR = 1.449, $P = 1.03 \times 10^{-15}$), AD (HR = 1.340, $P = 1.36 \times 10^{-5}$), vascular dementia (VD; HR = 1.763, $P = 5.84 \times 10^{-11}$), stroke (HR = 1.540, $P = 3.88 \times 10^{-23}$), anxiety (HR = 1.273, $P = 9.50 \times 10^{-11}$) and depression (HR = 1.429, $P = 1.56 \times 10^{-20}$). Plasma GFAP was significantly associated with risk of incident ACD (HR = 2.066, $P = 2.23 \times 10^{-76}$), AD (HR = 2.393, $P = 1.59 \times 10^{-71}$) and VD (HR = 2.281, $P = 4.66 \times 10^{-29}$). In addition, plasma LGALS4 level was mainly associated with higher risk of VD (HR = 1.571, $P = 5.52 \times 10^{-7}$), stroke (HR = 1.280, $P = 1.06 \times 10^{-9}$), anxiety (HR = 1.118, $P = 4.33 \times 10^{-4}$) and depression (HR = 1.239, $P = 2.69 \times 10^{-10}$). No significant associations were observed between KLK6, ADAM22 or CEACAM16 and any incident brain disorders. The full results are given in Supplementary Table 11.

In addition, we also tested the associations between BAG proteins and brain disorders regarding incidence time frame (Supplementary Fig. 10). Regarding short-term brain disorder

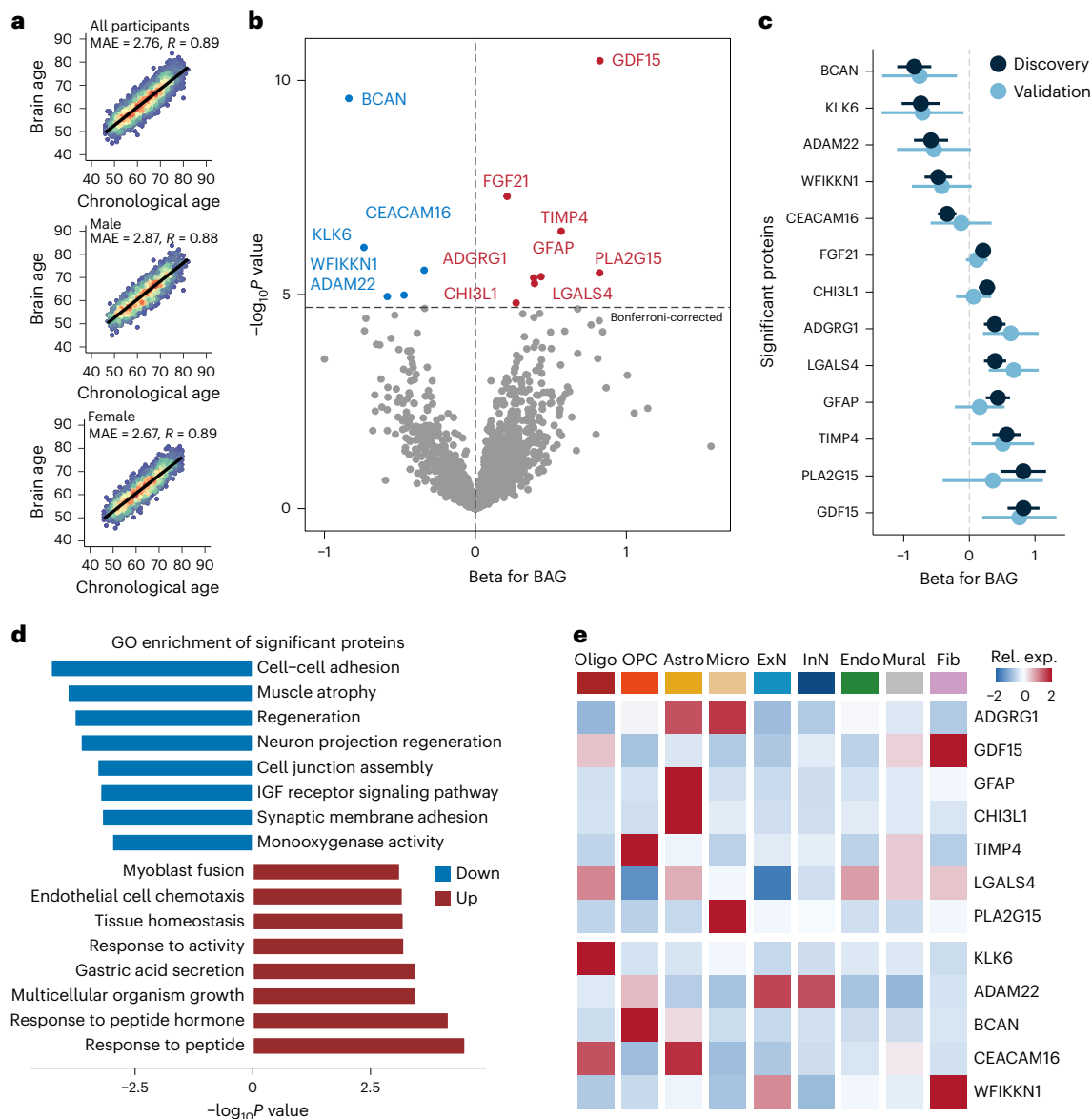


Fig. 2 | Protein-wide association of BAG. **a**, Prediction of brain age in the validation set using multimodal brain IDPs. Mean absolute error (MAE) and Pearson correlation coefficient between brain age (years) and chronological age (years) are shown in the top part of the plot. **b**, Volcano plot showing the results of protein-wide association analysis of BAG; proteins significantly associated with BAG are marked. Chronological age, sex, ethnicity, TDI, education level, smoking

status, alcohol status and body mass index were adjusted. Bonferroni correction was conducted for multiple corrections. **c**, Forest plot showing the results of discovery and validation analyses of the 13 BAG proteins. Error bars indicate s.e. **d**, The top representative biological processes of GO enrichment analyses. **e**, Relative expression (rel. exp.) levels of the 12 BAG protein-coding genes in different cell types of normal human brain. Mural, mural cell.

risk (occurring <5 years following protein measurement), BCAN (HR = 0.513, $P = 4.38 \times 10^{-4}$), GFAP (HR = 2.373, $P = 2.02 \times 10^{-23}$) and GDF15 (HR = 1.739, $P = 1.24 \times 10^{-7}$) remained significant with ACD. GFAP was the only significant protein associated with the risk of AD (HR = 3.322, $P = 4.49 \times 10^{-35}$), with GDF15 the only one associated with incident VD risk (HR = 2.161, $P = 1.65 \times 10^{-5}$). In addition to the identified significant associations with stroke, we found that CEACAM16 (HR = 0.783, $P = 2.87 \times 10^{-4}$) and FGF21 (HR = 1.141, $P = 2.63 \times 10^{-4}$) were significantly associated with short-term stroke risk. Regarding 10-year brain disorder risk, BCAN was significantly associated with incident ACD (HR = 0.599, $P = 1.16 \times 10^{-7}$). Both GFAP and GDF15 were still significantly associated with incident ACD (GFAP, HR = 2.246, $P = 8.01 \times 10^{-65}$; GDF15, HR = 1.573, $P = 2.53 \times 10^{-15}$), AD (GFAP, HR = 2.668, $P = 4.93 \times 10^{-62}$; GDF15, HR = 1.493, $P = 1.47 \times 10^{-6}$) and VD (GFAP, HR = 2.481, $P = 1.97 \times 10^{-21}$; GDF15, HR = 1.997, $P = 2.21 \times 10^{-10}$). Full details are given in Supplementary Tables 12 and 13.

Associations between BAG proteins and brain functions

Next, we tested the associations between BAG proteins and brain functions (Fig. 4b). Following Bonferroni correction, GDF15 was found to be associated with the highest number of brain functions, particularly BAG movement. However, only ten significant associations between BAG proteins and cognition were identified: five for GDF15, two for PLA2G15 and one for each of BCAN, TIMP4 and LGALS4.

Regarding mental health, both GDF15 and LGALS4 showed significant associations with the same six mental health traits. Moreover, both PLA2G15 and WFIKKN1 were also found to be closely related to mental health, with five significant associations. Full details are given in Supplementary Table 14.

Identification of specificity between BAG proteins and brain

We further used eight age-related disorders (infections, cancers, obesity, angina pectoris, myocardial infarction, asthma, inflammatory

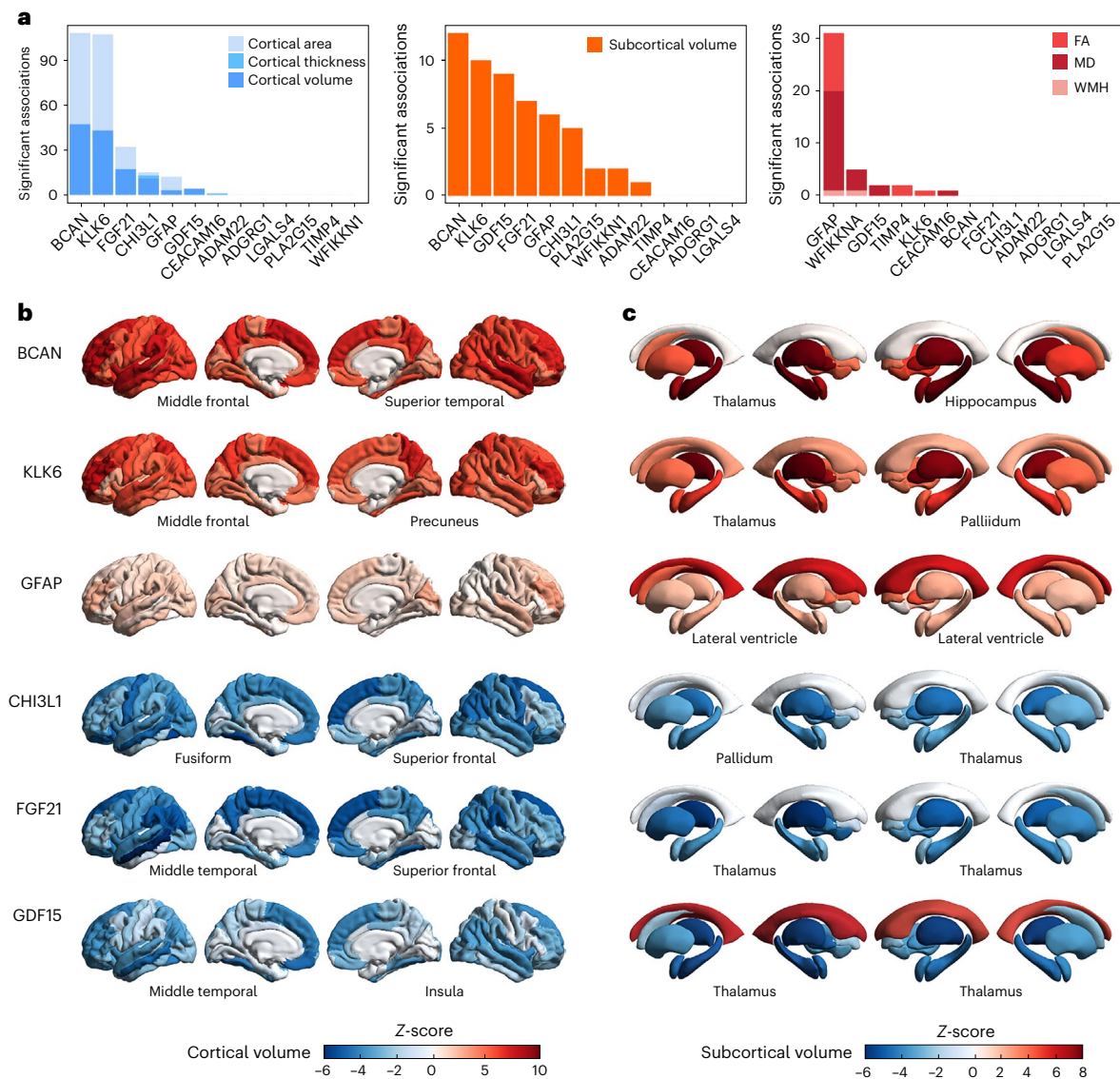


Fig. 3 | Associations between BAG proteins and brain structures. a, Bar plot showing the significant associations of 13 BAG proteins with cortical, subcortical and white matter structures. **b**, Associations between BAG proteins and cortical volume, tested using a linear regression model. **c**, Associations between BAG

proteins and subcortical volume, tested using a linear regression model. **b, c**, The most significant associations between protein and brain structure are indicated by z-score.

bowel disease and gout; Supplementary Table 15) to perform negative control analyses of the 13 BAG proteins. BCAN, GFAP and WFIKKN1 were not significantly associated with the age-related disorders of other systems (all $P > 4.81 \times 10^{-4}$). ADGRG1, ADAM22 and CEACAM16 were separately associated with one outcome, while GDF15 was associated with eight outcomes. Full details are given in Supplementary Table 16. Overall, these findings suggested that BCAN, GFAP and WFIKKN1 are specifically associated with brain-related traits.

Druggability assessment of BAG proteins

We conducted Mendelian randomization (MR) analysis between BAG proteins and BAG to test for causal associations (Supplementary Table 17). Genetically predicted plasma BCAN level was associated with lower BAG ($\beta = -0.473$, $P = 0.038$; Supplementary Fig. 11). Sensitivity analyses indicated neither heterogeneity ($P = 0.507$) nor pleiotropy ($P = 0.620$; Supplementary Table 18). However, no associations were identified between other BAG proteins and BAG (all $P > 0.05$; Supplementary Table 18). We further profiled the druggability of the 13 BAG proteins identified above (Supplementary Fig. 12). BCAN was found

to be a candidate druggable protein with moderate small-molecule druggability and high modality. Overall, these findings suggested that BCAN is a candidate druggable protein for brain aging.

Causalities between BAG proteins and brain health

For testing of causal associations between BAG proteins and brain health, we conducted MR analyses (Supplementary Table 17). These analyses supported the causal associations of BCAN with 13 cortical surface areas (all $P < 0.05$; Supplementary Table 19) and three cortical volumes (all $P < 0.05$). KLK6 was associated with four cortical surface areas (all $P < 0.05$) and left inferior temporal volume ($\beta = 0.047$, $P = 0.024$). Regarding white matter tracts, GFAP was associated with fractional anisotropy (FA) in left tract superior longitudinal fasciculus ($\beta = -0.151$, $P = 0.038$) and mean diffusivity (MD) in right tract posterior thalamic radiation ($\beta = 0.150$, $P = 0.045$). Regarding brain disorders, we identified the association between BCAN and PD ($\beta = -0.285$, $P = 0.032$; Supplementary Table 20). In regard to brain functions, GDF15 was negatively associated with normal walking pace ($\beta = -0.010$, $P = 0.043$; Supplementary Table 21).

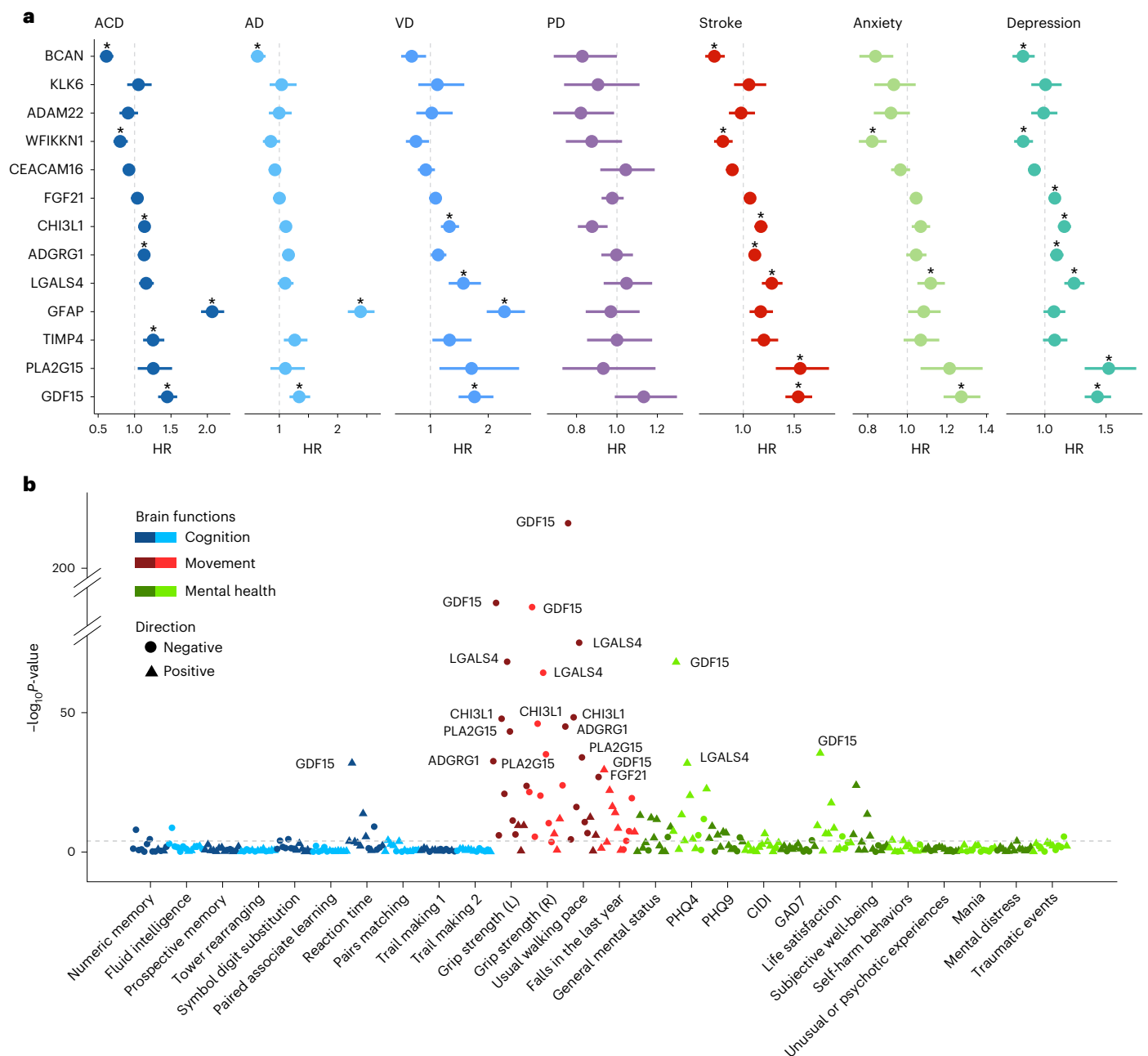


Fig. 4 | Associations between BAG proteins and brain disorders and brain functions. **a**, Forest plot showing the results of the association between BAG proteins and incident brain disorders. Significant associations following Bonferroni correction are marked by asterisks (*); error bars indicate s.e. **b**, Manhattan plot showing results of the association between BAG proteins and

brain functions. **a, b**, Chronological age, sex, ethnicity, TDI, education level, smoking status, alcohol status and body mass index were adjusted. Bonferroni correction was conducted for multiple corrections. Associations with $P < 1 \times 10^{-25}$ are marked. Dashed line indicates the threshold of adjusted P value (1.48×10^{-4}).

Undulating changes in plasma proteins during brain aging

Next, we sought to investigate undulating change patterns in plasma proteins with brain aging. The trajectories of 427 proteins nominally associated with BAG were profiled (Fig. 5a–c). We then performed unsupervised hierarchical clustering of these proteins (Supplementary Fig. 13), dividing them into six patterns with brain aging (Supplementary Table 22). As expected, we identified three clusters with linear patterns, clusters 1, 2 and 6 (Fig. 5d); the proteins of clusters 3 and 5 showed a logarithmic pattern. The normalized protein levels of cluster 3 peaked at approximately age 70 years (Fig. 5c), with the proteins of cluster 3 mainly associated with aneuploidy. Cluster 4 showed an inverted U-shaped pattern during brain aging, peaking around the sixth decade and then

decreasing (Fig. 5d). The proteins within cluster 4 were enriched for cell–cell adhesion. These findings suggested that, although most proteome changes across brain aging were linear, nearly one-third of plasma proteins showed a nonlinear pattern during brain aging.

Waves of brain aging-associated proteins

Due to the nonlinear patterns of plasma proteome alterations during brain aging identified above, we further performed differential expression-sliding window analysis (DE-SWAN) to quantify proteomic changes within a window of 2 years, by comparing groups in parcels of 1 year then sliding the window in increments of 1 year from young to old brain age. Three peaks of significant proteins at brain age 57,

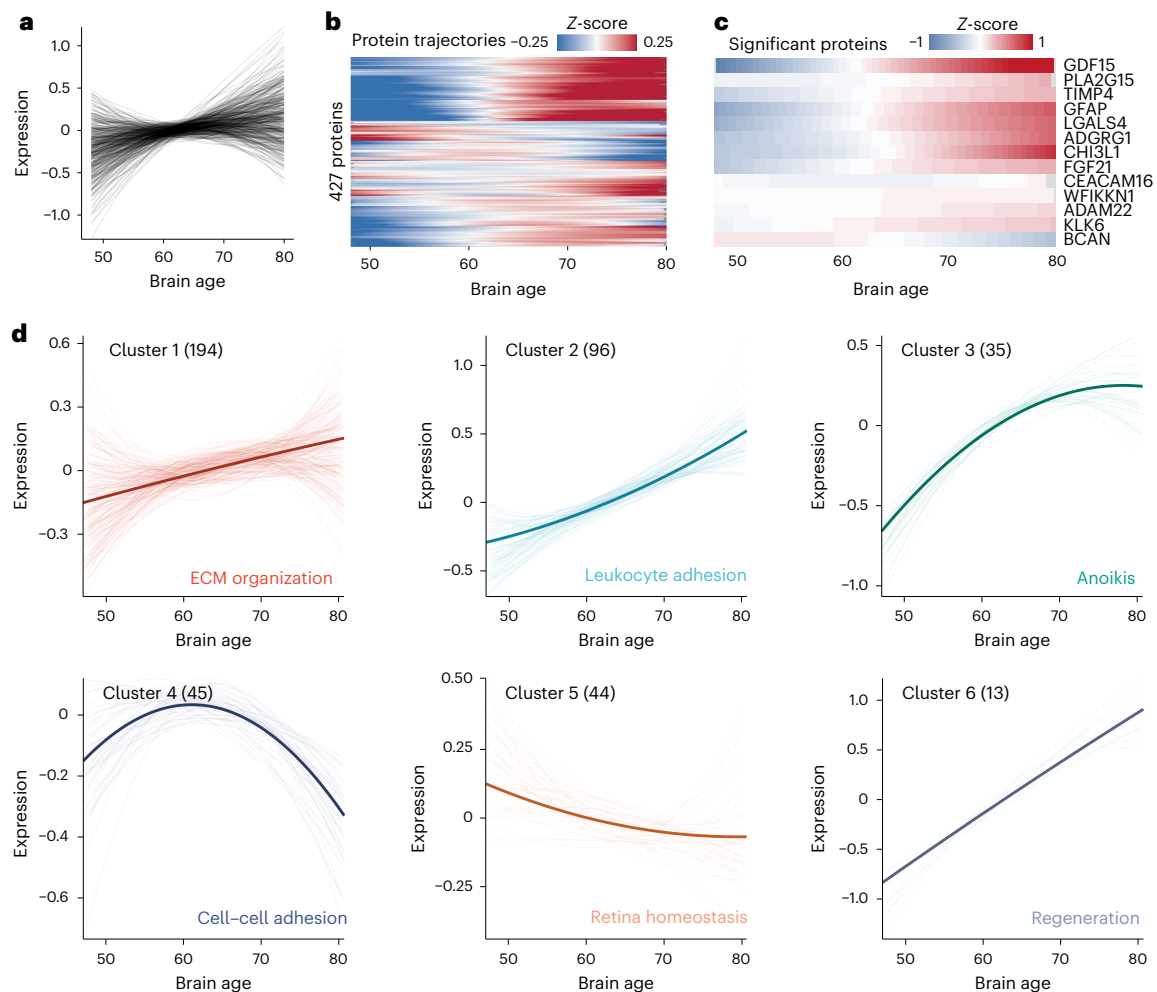


Fig. 5 | Undulating changes in plasma proteomes during brain aging.

a, Undulating changes in plasma proteins during brain aging (age in years). Plasma protein levels were z-scored and the changes in 427 plasma proteins estimated by LOESS. **b**, Heatmap showing undulating changes in 427 plasma proteins during brain aging. **c**, Heatmap showing undulating changes in the

13 BAG proteins during brain aging. **d**, Six clusters of plasma protein change patterns during brain aging. Thick lines represent the average trajectory for each cluster, with the top representative biological pathways of the cluster, and the number of proteins in parentheses.

70 and 78 years were detected (Figs. 6a and 5b). These peaks were still detectable with different thresholds of q -value, indicating the robustness of brain age-related waves (Supplementary Fig. 14 and Supplementary Table 23). The proteins of these peaks are given in Supplementary Table 24. Notably, we found that three brain age waves and BAG proteins generated by the linear model were largely different (Supplementary Fig. 15).

Biological pathways and implications of brain aging waves

At brain age 57 years, proteins were mainly associated with metabolic processes (Fig. 6c), while at brain age 70 years, protein waves were nominally associated with neuronal and developmental pathways. Regarding differential proteins at brain age 78, biological processes, including the JAK–STAT pathway, were identified. These findings indicated that brain age is an undulating process characterized by waves of changes in plasma proteomes that reflect complex shifts in biological processes.

We further tested associations between the proteins of all key wave and brain health traits, as well as inflammatory indices (Fig. 6d), finding that proteins at brain age wave 57 years showed most associations with mental health traits and PD. The highest number of associations between these proteins and adaptive immune markers was also observed. Moreover, we found that proteins at brain age wave 70 years

showed the highest number of associations with cognition, movement and brain structures; it is likely that these are also significantly associated with brain disorders, especially ACD and stroke. However, the associations between proteins at brain age wave 78 years and brain health traits were fewer than those for the other waves. Full details are given in Supplementary Tables 25–28. These findings indicated that brain age is an undulating process, characterized by waves of changes in plasma proteomes that reflect complex shifts in biological processes and implications for brain health.

Discussion

Our study integrated multimodal brain imaging and plasma proteomics data and investigated plasma proteome profiles across brain aging. We identified 13 plasma proteins associated with brain aging and validated six of them (GDF15, BCAN, TIMP4, KLK6, ADGRG1 and LGALS4). Their biological functions and implications for brain health were further characterized, and causal associations between these proteins and BAG were also tested, suggesting that BCAN is a candidate biomarker for brain aging. In addition, we uncovered the existence of undulating changes during brain aging, with proteomic alterations peaking in the late fifth, seventh and late seventh decades of brain age, suggesting that these are essential periods for intervention in the brain aging process.

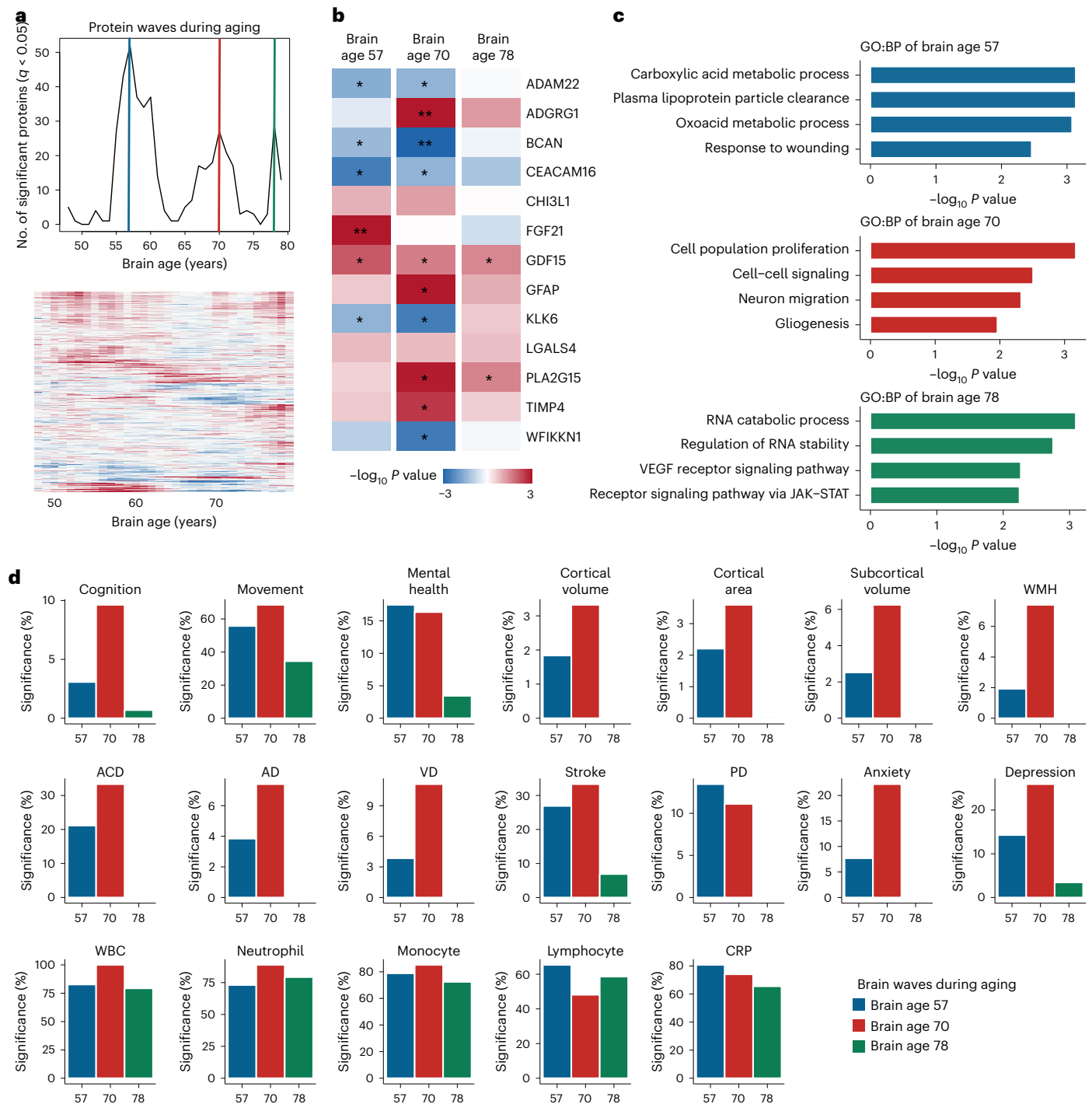


Fig. 6 | Plasma protein waves during brain aging. a, Top, the number of plasma proteins differentially expressed during brain aging. Three peaks, at brain age 57, 70 and 78 years, were observed. Bottom, plasma protein waves of brain aging. **b**, Heatmap showing the significance of the 13 BAG proteins at brain age 57, 70

and 78 years. * $P < 0.05$, ** $q < 0.05$. **c**, Top representative biological processes (BP) generated by GO enrichment of each protein wave. **d**, Barplots showing the proportions of significant associations between proteins of each brain age wave and phenotype. CRP, C-reactive protein; WBC, white blood cell count.

Previous studies have delineated candidate biomarkers of brain aging, encompassing discernible changes in DNA methylation²⁶ and histone modification²⁷. Regarding proteomics, Wingo et al. identified 579 proteins associated with cognitive trajectory²⁸, indicating that individuals with stable cognition in advanced age are characterized by increasing synaptic abundance and decreasing inflammation²⁸. However, their findings relied on the Mini-Mental State Examination, a coarse measurement of cognitive function²⁸ that may not accurately reflect brain health status more accurately than brain age derived from

brain MRI²⁹. To determine biomarkers of brain aging, three elements derived from physiological, medical imaging and humoral measurements are available to monitor the process of brain aging². These elements facilitate specific and pragmatic biomarkers of brain aging, and thus we propose a new brain age model based on multimodal brain imaging data. The relatively stable performance of our model underlines the robustness of subsequent analyses and findings. Our study profiled the landscape of plasma proteomics alterations during brain aging. We found decreasing synapse-related functions, but increasing

biological processes of extracellular matrix and stress-related pathways in brain aging, which is supported by a previous study²⁸. Dammer et al. analyzed AD plasma proteomes and demonstrated increasing extracellular matrix³⁰. Collectively, Johnson et al. investigated brain proteomes and identified an AD-associated protein module related to extracellular matrix³¹. The proteins associated with extracellular matrix are thus candidate therapeutic targets for brain aging. These findings are also supported by the imaging and histologic traits associated with brain aging, such as brain atrophy and loss of myelinated nerve fibers². We also found that the plasma proteins of brain aging have significant associations with brain health. BAG proteins are significantly associated with the frontal and temporal lobes, which are susceptible in aging and neurodegenerative disorders^{32,33}. These findings indicated the distinct significance of proteins in regard to region-specific brain structures. Plasma-based biomarkers are accessible, cost effective and minimally invasive, thus being suitable for early identification and monitoring of brain aging and related disorders³⁴. Previous studies have demonstrated that plasma A β 42, phosphorylated tau181 and neurofilament light chain levels have good predictive and discriminative values for AD^{35–37}. In addition, the plasma proteomics panel also demonstrated significant predictive value in regard to PD³⁸. The underlying mechanism linking plasma and brain aging is the pivotal contributions of peripheral immune processes³⁹. Peripheral immunity, including immune subtype abundance and inflammatory cytokines, is associated with aging and neurodegenerative disorders^{40,41}. Cerebral endothelial cells (Endo) are essential mediators of interactions between the periphery and brain. Yousef et al. demonstrated that aging blood upregulated VCAM1 in cerebral Endo, which activated microglia (Micro), reduced the activity of neural precursor cells and impaired cognition⁴². We identified the associations of plasma proteomes with brain aging and related traits of brain health, which suggested that plasma holds promise as a medium reflecting activities within the brain. However, further investigations are needed to determine whether plasma proteins could serve as an effective therapeutic target for mitigating the effects of brain aging.

Our study reports that BCAN is a biomarker of brain aging at both the protein and genetics level. *BCAN* was specifically expressed within the central nervous system⁴³, particularly in OPCs and Astro. BCAN is a neural proteoglycan involved in the perisynaptic extracellular matrix and synaptic plasticity in the brain⁴⁴. BCAN also regulates potassium channels and AMPA receptors, which control interneuronal plasticity and behavioral responses⁴⁵. BCAN expression in the hippocampus was found to be associated with spatial memory⁴⁶, while another study demonstrated that BCAN knockdown had a detrimental impact on long-term hippocampal CA1 potentiation⁴⁷. Associations of BCAN with several neurological disorders have been reported. Brevican was downregulated in a murine stroke model⁴⁸. Similarly, we found that baseline plasma BCAN levels predicted future stroke risk. Lower BCAN level was associated with cerebrovascular disease burden in cognitively impaired individuals without dementia⁴⁹. In addition, Minta et al. found that patients with VD had lower BCAN levels in cerebrospinal fluid than healthy controls or patients with AD⁵⁰. However, our study findings suggested that no association exists between BCAN and VD following multiple comparisons. Although the mechanisms underlying BCAN and brain aging were not revealed, alterations of extracellular matrix during aging partly explained the association. Extracellular matrix within brain parenchyma was found to be involved in neuronal plasticity, learning and memory⁵¹, and its expression, composition, location and physical properties underwent substantial alterations in aging^{25,52}, with notable influence on neural and glial functions⁴⁸. Extracellular matrix components also induced neuroinflammatory responses in the aging brain⁵³. In addition, BCAN is an essential proteoglycan of perineuronal nets (PNNs) of the extracellular matrix. However, both BCAN and PNNs underwent degradation and decomposition in human postmortem AD brains⁵⁴. Notably, neurites associated with PNNs were spared from

tau pathology and no BCAN was detected within amyloid plaques⁵⁴. In general, our study suggested that BCAN is a candidate for brain aging and related brain disorders, but the underlying mechanisms require further investigation.

Our study also provided several candidate biomarkers for brain aging. GDF15 was found to be the most significant plasma protein associated with brain aging in our analysis, and was also associated with chronological age²² and multiple age-related disorders^{55,56}. Notably, previous studies have demonstrated the association of GDF15 with future ACD^{57,58}, highlighting its significant role in neurodegenerative disorders. GDF15 is a stress-regulated hormone and was upregulated in response to environmental stress, being involved in energy homeostasis, insulin resistance^{59–61} and mitochondrial dysfunction⁶². Although several studies reported the anti-inflammatory functions of GDF15 (ref. 63), it is an essential component of the senescence-associated secretory phenotype⁶⁴, which promotes neuroinflammation, synaptic dysfunction, neuropathological changes, neuronal death and, ultimately, cognitive impairment⁶⁵. Notably, due to the significant associations of GDF15 with age and age-related disease, and its ubiquitous expression in the human body, GDF15 is a more probable general biomarker of aging⁶⁶ but not one specific for brain aging. In addition to GDF15, KLK6 is a protease within the central nervous system and is mainly associated with functioning of the blood–brain barrier and Oligo^{67,68}. Although Mitsui et al. suggested that lower KLK6 levels in cerebrospinal fluid are associated with AD, other studies reported inconsistent results^{69,70}. Therefore, the association between the proteins identified in our study and brain aging requires further investigation.

Another key finding of our study is the undulating plasma proteomic changes throughout the process of brain aging. We identified three essential protein waves associated with brain age at 57, 70 and 78 years. However, the proteins of these peaks have minimal overlap in components and functional enrichment. In contrast to the general biological aging process, we found that the late fifth decade is a potential onset time point for brain aging, showed the most differential proteins, and is characterized by response to wounding and metabolic processes. Hahn et al. conducted spatiotemporal transcriptomic analyses of aging murine brain and demonstrated that the majority of brain regions exhibited substantial transcriptomic differences at approximately 18 months (equivalent to 56 years in humans)⁷¹, which supports our findings. We also found that a majority of these proteins are associated with adaptive immunity, which is a potential mechanism of brain aging during this period. In addition, our study suggested that the seventh and late seventh decades are also essential time points in brain aging, aligning with observed waves in the aging plasma proteome²². Similarly, a large-scale cerebrospinal fluid scRNA sequencing (scRNA-seq) study identified the peak of differential expression genes for most cell types at 78 years⁷². Moreover, Fujita et al. profiled brain volume changes during aging in cognitively unimpaired individuals and found that the rate of brain atrophy accelerated from about 70 years⁷³. Characterization of undulating changes in the brain aging plasma proteome carry great significance for personalized prevention of, and intervention in, brain aging and subsequent age-related brain disorders. For instance, we found that proteins at the seventh decade showed most associations with age-related brain disorders; indeed, the prevalence of neurodegenerative disorders such as AD and PD increased significantly in people aged >70 years⁴. Our findings thus emphasize the importance and necessity of intervention and prevention at brain age 70 years to reduce the risk of multiple brain disorders. In addition, we found that proteins associated with the JAK–STAT signaling pathway differentially expressed at brain age 78 years. Xu et al. demonstrated that inhibition of JAK rescued senescence-associated secretory phenotype and frailty. The upregulation of proteins associated with the JAK–STAT pathway in the late seventh decade of brain age may therefore further exacerbate the degree of brain aging, and inhibition of the JAK–STAT pathway is a candidate intervention for advanced brain aging⁷⁴. Overall, these findings

indicate that the pace of brain aging is uneven across the lifespan, and further studies are warranted to elucidate the underlying mechanisms of certain proteins at different stages of brain aging.

The strengths of our study include the integration of multimodal brain imaging data and plasma proteomics in a large community-based cohort. In addition, we tested nonlinear changes during brain aging, a factor occasionally overlooked in previous studies. However, some limitations should be noted. First, the participants in our study were middle-aged and older adults; a cohort covering the entire lifespan is required to gain a more comprehensive understanding of the undulating changes in brain aging. Therefore, the undulating changes in brain age occurring before 40 years need to be further explored. Second, because the UK Biobank participants were mainly of European ancestry, the results of our study should be further validated in cohorts of other ethnicities. One further limitation is that plasma-based assays mainly focus on immunity-related secreted proteins and thus over-represent biological processes such as immune responses while under-representing others, including mitochondrial function and neuronal network activity. Therefore, brain-based analyses with larger sample size are warranted to give an unbiased picture of the relative importance of different proteins or pathways in regard to brain aging. Moreover, it should be noted that our protein-wide association analysis was based on 2,922 plasma proteins provided by the Olink platform. These proteins do not encompass the entire human proteome, and some underlying molecular mechanisms probably remain obscured. In addition, to avoid sample overlap in MR analyses, we obtained plasma proteome Genome-Wide Association Study (GWAS) data from the deCODE consortium, which uses the Somascan V4 platform. It should also be acknowledged that, although moderate assay variance and genetic correlation were identified between the Somascan and Olink platforms, the former identified fewer protein quantitative trait loci and genomic associations than the latter⁷⁵, which probably affected the results of MR analyses. However, roughly 500 proteins had protein quantitative trait loci on both platforms and there was a strong correlation between protein levels measured by the two platforms. Overall, the results of MR analyses require further investigation.

In summary, our study provides insights into plasma proteomic alterations during brain aging. Importantly, we identified BCAN as a promising biomarker for brain aging and pinpointed 57, 70 and 78 years as transitional time points during brain aging. These findings contribute to bridging essential knowledge gaps in clarifying the molecular mechanisms of brain aging, with substantial implications for the future development of systemic and pragmatic biomarkers for brain aging, as well as personalized therapeutic targets for subsequent age-related brain disorders.

Methods

Ethics statement

This study adhered to the Declaration of Helsinki. All individuals gave written informed consent at baseline, and approval of the study was obtained from the North West Multi-Center Research Ethics Committee (no. 11/NW/0382).

Study participants

The participants included in the present study were from UK Biobank, a large-scale prospective cohort with >500,000 community dwellers from 22 assessment centers throughout the United Kingdom, the study being in operation between 2006 and 2010 (ref. 76). The demographic characteristics, biological samples and physical measurements of each participant were obtained at recruitment, and all participants were registered with the UK National Health Service.

Brain imaging-derived phenotypes

At the imaging visit (around 4 years following recruitment assessment), the brain imaging data of >40,000 participants from UK Biobank were

obtained on a standard Siemens Skyra 3 T scanner with a 32-channel head coil⁷⁷. The parameters were previously demonstrated⁷⁷, and the protocol of brain imaging, including image processing pipeline, artifact removal, cross-modality and cross-individual image alignment, quality control and phenotype calculation, is accessible through the website https://biobank.ndph.ox.ac.uk/showcase/showcase/docs/brain_mri.pdf.

Following screening, we excluded IDPs with low sample size (that is, arterial spin labeling data covering <20% of all participants); reduplicated IDPs (that is, cortical structures generated by a different segmentation approach) and 1,705 unique brain IDPs with high coverage (>80% of all participants) remained in brain age model development, including:

- structural imaging ($n = 1,181$): T1-weighted structural brain imaging and T2-weighted brain imaging
- functional imaging ($n = 60$): task functional brain MRI and resting-state functional brain imaging
- susceptibility-weighted brain imaging ($n = 32$): magnetic susceptibility and T2star
- diffusion imaging ($n = 432$): diffusion MRI (dMRI) skeleton measurement

Although some IDPs were overlapping (that is, surface area and volume of the same region) and hierarchically related (total volume white matter hyperintensities (WMH), deep WMH and periventricular WMH), they reflected different aspects of the aging brain^{71,78}. Details of the included brain IDPs are presented in Supplementary Table 1.

Development of multimodal brain age model

Following the selection of brain IDPs, at the imaging visit we further excluded those with neuropsychiatric and related disorders (for example, hypertension, atherosclerosis, emphysema and gout; see Supplementary Table 2 for complete details). Moreover, to increase statistical power in protein-wide association analysis, we restricted it to those without plasma proteomics data in model development. Finally, 10,000 healthy participants with brain IDP data, but without plasma proteomics data, remained (Supplementary Fig. 1), and these participants were further divided into a training set (70%) and a testing set (30%). LASSO regression was used to develop multimodal brain age, due to its superior performance compared with other machine learning models⁷⁹. The LASSO algorithm can select those feature variables having a significant impact on the target variable while maintaining prediction accuracy, thus reducing both model complexity and the impact of overlapping measures on prediction of brain age. Brain IDP data and chronological age at the imaging visit were used to train the multimodal brain age model. The parameter λ was optimized using tenfold cross-validation to achieve minimal deviance, which is a measure of the goodness of fit.

Proteomics data

Over 50,000 participants were included in the UK Biobank Pharma Proteomics Project. Blood samples were collected at the recruitment visit and plasma samples isolated by centrifugation. Plasma proteomics were examined and quantified through the Olink Explore Proximity Extension Assay platform, which measured 2,923 unique proteins. Experimenting investigators were blinded to all sample characteristics and clinical data, and data collection and analysis were not performed blind to the conditions of the experiments. Following quality control, normalization and batch effect correction, normalized protein expression values were generated⁷⁵.

Statistics and reproducibility

For identification of proteins associated with brain aging, we calculated brain age in participants using both brain IDPs and plasma proteomics data ($n = 4,696$) and further calculated BAG, the deviance of predicted

brain age and chronological age (Supplementary Fig. 1). The linear regression model was used to identify BAG-associated proteins. Potential confounding factors, including chronological age, sex, ethnicity, Townsend's deprivation index (TDI), education level, smoking status, alcohol status and body mass index, were adjusted in the model. Bonferroni correction was conducted for multiple corrections.

To provide confidence in the reproducibility of protein-wide association analysis, we utilized brain IDP data at the repeat imaging visit to calculate BAG, and conducted further protein-wide association analyses. Those proteins nominally with BAG ($P < 0.05$) were considered significant in the validation analysis.

No statistical method was used to predetermine sample size, but our sample size was similar to that in a study reported in a previous publication²². In addition, data distribution was assumed to be normal, but this was not formally tested.

Functional enrichment of proteins

Functional enrichment analyses, including Gene Ontology (GO) of proteins surviving following false discovery rate correction, were conducted using the R package clusterProfiler, with default parameters⁸⁰. Proteins listed in the Olink Explore 3072 platform by the UKB Pharma Proteomics Project were used as background. The results were adjusted for multiple comparisons using the Benjamini–Hochberg method. Terms or pathways with adjusted $P < 0.05$ were defined as enrichment. The top representative biological processes or pathways were visualized using the R package ggpubr.

Single-cell transcriptome data and expression-based analysis

Single-cell transcriptomic data were used to test the expression levels of protein-coding genes in different cell types. We obtained normal human brain snRNA-seq data from Garcia et al. to identify expression levels in major cell types within the brain⁸¹, which included 61,862 individual cells from 17 samples. Samples were obtained from Boston Children's Hospital through the Repository Core for Neurological Disorders; all participants were between 11 and 22 years of age and had a primary diagnosis of medically refractory epilepsy with no known genetic mutations. We also obtained human peripheral blood mononuclear cell scRNA-seq data from ten young and seven old individuals from Zhu et al., to test their expression levels in peripheral blood⁸². These individuals were from the Shanghai East Hospital natural aging cohort, and were generally healthy at the time of blood collection according to evaluation of medical history and assessment of vital signs. To test whether expression levels of protein-coding genes were altered in neurodegenerative disorders, we obtained prefrontal cortex snRNA-seq data from patients with late-stage AD ($n = 11$) and age-matched cognitively healthy controls ($n = 7$) from Morabito et al.⁸³. These samples were obtained from the University of California, Irvine Memory Impairments and Neurological Disorders' Alzheimer's Disease Research Center tissue repository and under the University of California Institutional Review Board, with diagnosis based on Braak and plaque staging. Details on single-cell transcriptomic data are given in Supplementary Table 8. The R package Seurat was used for key data analysis and visualization⁸⁴, and the R package harmony for data integration and batch effect correction⁸⁵.

Brain health traits

Brain health was categorized into three major groups: brain disorders, brain functions and brain structures. Details of brain health traits are given in Supplementary Table 9. Primary brain disorders in this study included all-cause dementia, AD, VD, PD, stroke, anxiety and depression. Diagnosis of brain disorders was coded based on International Classification of Diseases, Tenth Revision. Those with corresponding brain disorders at baseline were excluded from analysis. The endpoint of follow-up was determined by either the first occurrence of the brain disorder, date of death or end of follow-up (30 June 2023), whichever occurred first. In regard to brain functions, we mainly focused on

cognition ($n = 10$), movement ($n = 4$) and mental health ($n = 12$). To identify the associations between BAG-associated proteins and fine brain structures, the volume, area and thickness of 68 unique cortical regions, the volume of 16 subcortical regions and the weighted median FA and MD of 27 white matter tracts were obtained.

The Cox proportional model was used to test associations between BAG-associated proteins surviving following Bonferroni correction and incident brain disorders. The linear regression model was used to identify associations between BAG-associated proteins surviving following Bonferroni correction and brain functions and structures. Potential confounding factors, including chronological age, sex, ethnicity, TDI, education level, smoking status, alcohol status and body mass index, were adjusted in the model. In regard to dementia outcomes (all-cause dementia, AD and VD), *APOE-ε4* status, which was defined as the number of *APOE-ε4* alleles, was further adjusted. Regarding incidence time frame analysis, we repeated the above analyses among these target populations: 5- and 10-year incident brain disorder. When conducting incidence time frame analyses, individuals who developed a specific brain disorder following the time stamps were treated as healthy individuals. Bonferroni correction (only significant proteins associated with BAG were considered) was conducted for multiple corrections.

Negative control analyses of proteins with BAG

Negative control analyses were aimed at testing whether proteins were specifically associated with brain-related traits. A total of eight age-related, but not brain-related, disorders in negative control analyses were considered: infections, cancers, obesity, angina pectoris, myocardial infarction, asthma, inflammatory bowel disease and gout (Supplementary Table 15 provides complete details). The Cox proportional model was used to test associations, and chronological age, sex, ethnicity, TDI, education level, smoking status, alcohol status and body mass index were adjusted in the model. Bonferroni correction (only significant proteins associated with BAG were considered) was conducted for multiple corrections.

Druggability of proteins associated with BAG

The druggability of proteins associated with BAG was profiled, leveraging agora druggability and ligandability analysis using the Accelerating Medicines Partnership for Alzheimer's Disease consortium (<https://www.synapse.org/#!/Synapse:syn13363443>). Proteins were scored for their suitability as drug targets. Briefly, proteins were placed in buckets that were ordered based on the preference for small-molecule drug development, therapeutic antibody feasibility and safety, with lower-numbered buckets being generally accepted as easier or more likely to result in successful drug development than higher-numbered buckets.

Mendelian randomization

For testing of causal associations between plasma proteins and BAG and brain-related traits, two-sample MR analysis was performed. MR analyses rely on the use of instrumental variables (IVs), and there are three major assumptions included: (1) IVs are significantly associated with exposure; (2) IVs are not associated with confounding factors; and (3) IVs are associated with the outcome indirectly through exposure⁸⁶.

For selection of IVs, we first identify those single-nucleotide polymorphisms (SNPs) significantly associated with the plasma protein ($P < 1 \times 10^{-6}$). Those SNPs located within the major histocompatibility complex and those with minor allele frequency < 0.01 were removed. Next, linkage disequilibrium was tested among SNPs at the threshold of $r^2 < 0.001$ and a window of 10,000 base pairs. In regard to plasma protein GWAS data, to avoid sample overlap, plasma proteomics GWAS data from the deCODE consortium were obtained⁸⁷. For BAG GWAS data, we obtained summary-level BAG GWAS data from Leonardsen et al.¹⁹, which were generated from 28,104 individuals from UK Biobank. Details of GWAS data on brain-related traits are given in Supplementary Table 17.

In MR analysis, the inverse-variance weighted method was used to pool the estimate of each SNP, to generate a combined and consistent estimate of the effect of exposure on outcome, and this was used as the main analysis⁸⁸. Cochran's *Q* test and the Egger intercept test were used for heterogeneity and pleiotropy testing, respectively. All MR analyses were conducted using the R package TwoSampleMR⁸⁹. Associations with $P < 0.05$ were considered causal.

Undulating changes in proteins during brain aging

A total of 427 proteins nominally associated ($P < 0.05$) with BAG were selected for estimation of undulating changes in proteins during brain aging. First, protein levels were *z*-normalized, then a LOESS regression of span of 300 was used to fit each plasma protein with brain age. Pairwise differences between LOESS estimates were calculated through Euclidian distance, and hierarchical clustering using a complete method was subsequently conducted to group the different patterns into six clusters for brain aging. The corresponding biological pathways of each cluster were further inferred with GO databases as described above. Biological processes with adjusted $P < 0.05$ were considered significant.

DE-SWAN

The DE-SWAN method was used to identify and quantify nonlinear changes in plasma proteome during brain aging with the R package DEswan²². First, the brain age of healthy participants was rounded, restricting the range to those aged 47–81 years. Thus, 34 centers with windows of ± 1 year were used. In regard to differential expression analysis, the following model was used:

$$\text{Protein level} \sim \alpha + \beta_1 \text{ brain age}_{\text{low/high}} + \beta_2 \text{sex} + \beta_3 \text{ethnicity} + \dots + \varepsilon$$

The *q*-values of each brain age wave were estimated by Benjamini–Hochberg correction. Type II sum of squares was calculated using the analysis of variance function in the R package car. Proteins with $q < 0.05$ were considered significant.

Reporting summary

Further information on research design is available in the Nature Portfolio Reporting Summary linked to this article.

Data availability

The data used in this study are available from UK Biobank, with restrictions applied, under application no. 19542. Access to UK Biobank data can be requested through a standard protocol via their website (<https://www.ukbiobank.ac.uk/register-apply/>).

Code availability

This study used open-source software and codes, specifically R (<https://www.r-project.org/>), glmnet (<https://github.com/cran/glmnet>), clusterProfiler (<https://github.com/YuLab-SMU/clusterProfiler>), Seurat (<https://satijalab.org/seurat>), harmony (<https://github.com/immunogenomics/harmony>), TwoSampleMR (<https://github.com/MRCIEU/TwoSampleMR>) and DEswan (<https://github.com/lehallier/DEswan>).

References

- Cai, Y. et al. The landscape of aging. *Sci. China Life Sci.* **65**, 2354–2454 (2022).
- Aging Biomarker Consortium et al. Biomarkers of aging. *Sci. China Life Sci.* **66**, 893–1066 (2023).
- Fratiglioni, L., Marseglia, A. & Dekhtyar, S. Ageing without dementia: can stimulating psychosocial and lifestyle experiences make a difference? *Lancet Neurol.* **19**, 533–543 (2020).
- Hou, Y. et al. Ageing as a risk factor for neurodegenerative disease. *Nat. Rev. Neurol.* **15**, 565–581 (2019).
- Mattson, M. P. & Arumugam, T. V. Hallmarks of brain aging: adaptive and pathological modification by metabolic states. *Cell Metab.* **27**, 1176–1199 (2018).
- Cai, W. et al. Dysfunction of the neurovascular unit in ischemic stroke and neurodegenerative diseases: an aging effect. *Ageing Res. Rev.* **34**, 77–87 (2017).
- Fox, N. C. & Schott, J. M. Imaging cerebral atrophy: normal ageing to Alzheimer's disease. *Lancet* **363**, 392–394 (2004).
- Tarumi, T. et al. Cerebral hemodynamics in normal aging: central artery stiffness, wave reflection, and pressure pulsatility. *J. Cereb. Blood Flow Metab.* **34**, 971–978 (2014).
- Riddle, D. R., Sonntag, W. E. & Lichtenwalner, R. J. Microvascular plasticity in aging. *Ageing Res. Rev.* **2**, 149–168 (2003).
- Zhang, H. et al. Single-nucleus transcriptomic landscape of primate hippocampal aging. *Protein Cell* **12**, 695–716 (2021).
- Baecker, L., Garcia-Dias, R., Vieira, S., Scarpazza, C. & Mechelli, A. Machine learning for brain age prediction: introduction to methods and clinical applications. *EBioMedicine* **72**, 103600 (2021).
- Cole, J. H. & Franke, K. Predicting age using neuroimaging: innovative brain ageing biomarkers. *Trends Neurosci.* **40**, 681–690 (2017).
- Lee, J. et al. Deep learning-based brain age prediction in normal aging and dementia. *Nat. Aging* **2**, 412–424 (2022).
- Millar, P. R. et al. Advanced structural brain aging in preclinical autosomal dominant Alzheimer disease. *Mol. Neurodegener.* **18**, 98 (2023).
- Beheshti, I., Mishra, S., Sone, D., Khanna, P. & Matsuda, H. T1-weighted MRI-driven brain age estimation in Alzheimer's disease and Parkinson's disease. *Ageing Dis.* **11**, 618–628 (2020).
- Han, L. K. M. et al. Brain aging in major depressive disorder: results from the ENIGMA major depressive disorder working group. *Mol. Psychiatry* **26**, 5124–5139 (2021).
- Schnack, H. G. et al. Accelerated brain aging in schizophrenia: a longitudinal pattern recognition study. *Am. J. Psychiatry* **173**, 607–616 (2016).
- Liew, S.-L. et al. Association of brain age, lesion volume, and functional outcome in patients with stroke. *Neurology* **100**, e2103–e2113 (2023).
- Leonardsen, E. H. et al. Genetic architecture of brain age and its causal relations with brain and mental disorders. *Mol. Psychiatry* **28**, 3111–3120 (2023).
- Walker, K. A. et al. Large-scale plasma proteomic analysis identifies proteins and pathways associated with dementia risk. *Nat. Aging* **1**, 473–489 (2021).
- Tanaka, T. et al. Plasma proteomic signature of age in healthy humans. *Ageing Cell* **17**, e12799 (2018).
- Lehallier, B. et al. Undulating changes in human plasma proteome profiles across the lifespan. *Nat. Med.* **25**, 1843–1850 (2019).
- Guest, P. C., Guest, F. L. & Martins-de Souza, D. Making sense of blood-based proteomics and metabolomics in psychiatric research. *Int. J. Neuropsychopharmacol.* **19**, pyv138 (2016).
- Bieri, G., Schroer, A. B. & Villeda, S. A. Blood-to-brain communication in aging and rejuvenation. *Nat. Neurosci.* **26**, 379–393 (2023).
- Oh, H. S.-H. et al. Organ aging signatures in the plasma proteome track health and disease. *Nature* **624**, 164–172 (2023).
- Chouliaras, L. et al. Age-related increase in levels of 5-hydroxymethylcytosine in mouse hippocampus is prevented by caloric restriction. *Curr. Alzheimer Res.* **9**, 536–544 (2012).
- Peleg, S. et al. Altered histone acetylation is associated with age-dependent memory impairment in mice. *Science* **328**, 753–756 (2010).
- Wingo, A. P. et al. Large-scale proteomic analysis of human brain identifies proteins associated with cognitive trajectory in advanced age. *Nat. Commun.* **10**, 1619 (2019).

29. Tian, Y. E. et al. Heterogeneous aging across multiple organ systems and prediction of chronic disease and mortality. *Nat. Med.* **29**, 1221–1231 (2023).
30. Dammer, E. B. et al. Multi-platform proteomic analysis of Alzheimer's disease cerebrospinal fluid and plasma reveals network biomarkers associated with proteostasis and the matrisome. *Alzheimers Res Ther.* **14**, 174 (2022).
31. Johnson, E. C. B. et al. Large-scale deep multi-layer analysis of Alzheimer's disease brain reveals strong proteomic disease-related changes not observed at the RNA level. *Nat. Neurosci.* **25**, 213–225 (2022).
32. DeCarli, C. et al. Measures of brain morphology and infarction in the Framingham Heart Study: establishing what is normal. *Neurobiol. Aging* **26**, 491–510 (2005).
33. Scheltens, P. et al. Alzheimer's disease. *Lancet* **397**, 1577–1590 (2021).
34. Klyucherev, T. O. et al. Advances in the development of new biomarkers for Alzheimer's disease. *Transl. Neurodegener.* **11**, 25 (2022).
35. Cai, H., Pang, Y., Fu, X., Ren, Z. & Jia, L. Plasma biomarkers predict Alzheimer's disease before clinical onset in Chinese cohorts. *Nat. Commun.* **14**, 6747 (2023).
36. Chatterjee, P. et al. Plasma A β 42/40 ratio, p-tau181, GFAP, and NfL across the Alzheimer's disease continuum: a cross-sectional and longitudinal study in the AIBL cohort. *Alzheimers Dement.* **19**, 1117–1134 (2023).
37. Guo, Y. et al. The dynamics of plasma biomarkers across the Alzheimer's continuum. *Alzheimers Res. Ther.* **15**, 31 (2023).
38. Hällqvist, J. et al. Plasma proteomics identify biomarkers predicting Parkinson's disease up to 7 years before symptom onset. *Nat. Commun.* **15**, 4759 (2024).
39. Bettcher, B. M., Tansey, M. G., Dorothée, G. & Heneka, M. T. Peripheral and central immune system crosstalk in Alzheimer disease - a research prospectus. *Nat. Rev. Neurol.* **17**, 689–701 (2021).
40. Zenaro, E. et al. Neutrophils promote Alzheimer's disease-like pathology and cognitive decline via LFA-1 integrin. *Nat. Med.* **21**, 880–886 (2015).
41. Wang, P. et al. Single-cell transcriptome and TCR profiling reveal activated and expanded T cell populations in Parkinson's disease. *Cell Discov.* **7**, 52 (2021).
42. Yousef, H. et al. Aged blood impairs hippocampal neural precursor activity and activates microglia via brain endothelial cell VCAM1. *Nat. Med.* **25**, 988–1000 (2019).
43. Yamaguchi, Y. Brevican: a major proteoglycan in adult brain. *Perspect. Dev. Neurobiol.* **3**, 307–317 (1996).
44. Frischknecht, R. & Seidenbecher, C. I. Brevican: a key proteoglycan in the perisynaptic extracellular matrix of the brain. *Int. J. Biochem. Cell Biol.* **44**, 1051–1054 (2012).
45. Favuzzi, E. et al. Activity-dependent gating of parvalbumin interneuron function by the perineuronal net protein brevican. *Neuron* **95**, 639–655 (2017).
46. Saroja, S. R. et al. Hippocampal proteoglycans brevican and versican are linked to spatial memory of Sprague-Dawley rats in the Morris water maze. *J. Neurochem.* **130**, 797–804 (2014).
47. Brakebusch, C. et al. Brevican-deficient mice display impaired hippocampal CA1 long-term potentiation but show no obvious deficits in learning and memory. *Mol. Cell. Biol.* **22**, 7417–7427 (2002).
48. Chmelova, M. et al. A view of the genetic and proteomic profile of extracellular matrix molecules in aging and stroke. *Front. Cell. Neurosci.* **17**, 1296455 (2023).
49. Chia, R. S. L. et al. Serum brevican as a biomarker of cerebrovascular disease in an elderly cognitively impaired cohort. *Biomolecules* **14**, 75 (2024).
50. Minta, K. et al. Brevican and neurocan peptides as potential cerebrospinal fluid biomarkers for differentiation between vascular dementia and Alzheimer's disease. *J. Alzheimers Dis.* **79**, 729–741 (2021).
51. Fatemi, S. H. Reelin glycoprotein: structure, biology and roles in health and disease. *Mol. Psychiatry* **10**, 251–257 (2005).
52. Hußler, W. et al. Brevican and neurocan cleavage products in the cerebrospinal fluid - differential occurrence in ALS, epilepsy and small vessel disease. *Front. Cell. Neurosci.* **16**, 838432 (2022).
53. Deleidi, M., Jäggle, M. & Rubino, G. Immune aging, dysmetabolism, and inflammation in neurological diseases. *Front. Neurosci.* **9**, 172 (2015).
54. Morawski, M. et al. Involvement of perineuronal and perisynaptic extracellular matrix in Alzheimer's disease neuropathology. *Brain Pathol.* **22**, 547–561 (2012).
55. You, J. et al. Plasma proteomic profiles predict individual future health risk. *Nat. Commun.* **14**, 7817 (2023).
56. Baek, S. J. & Eling, T. Growth differentiation factor 15 (GDF15): a survival protein with therapeutic potential in metabolic diseases. *Pharmacol. Ther.* **198**, 46–58 (2019).
57. Walker, K. A. et al. Proteomics analysis of plasma from middle-aged adults identifies protein markers of dementia risk in later life. *Sci. Transl. Med.* **15**, eadf5681 (2023).
58. Guo, Y. et al. Plasma proteomic profiles predict future dementia in healthy adults. *Nat. Aging* **4**, 247–260 (2024).
59. Tsai, V. W. W., Husaini, Y., Sainsbury, A., Brown, D. A. & Breit, S. N. The MIC-1/GDF15-GFRAL pathway in energy homeostasis: implications for obesity, cachexia, and other associated diseases. *Cell Metab.* **28**, 353–368 (2018).
60. Lockhart, S. M., Saudek, V. & O'Rahilly, S. GDF15: a hormone conveying somatic distress to the brain. *Endocr. Rev.* **41**, bnaa007 (2020).
61. Kim, J. et al. TFEB-GDF15 axis protects against obesity and insulin resistance as a lysosomal stress response. *Nat. Metab.* **3**, 410–427 (2021).
62. Wedel, S. et al. Depletion of growth differentiation factor 15 (GDF15) leads to mitochondrial dysfunction and premature senescence in human dermal fibroblasts. *Aging Cell* **22**, e13752 (2023).
63. Kempf, T. et al. GDF-15 is an inhibitor of leukocyte integrin activation required for survival after myocardial infarction in mice. *Nat. Med.* **17**, 581–588 (2011).
64. Basisty, N. et al. A proteomic atlas of senescence-associated secretomes for aging biomarker development. *PLoS Biol.* **18**, e3000599 (2020).
65. Gaikwad, S., Senapati, S., Haque, M. A. & Kaye, R. Senescence, brain inflammation, and oligomeric tau drive cognitive decline in Alzheimer's disease: evidence from clinical and preclinical studies. *Alzheimers Dement.* **20**, 709–727 (2024).
66. Conte, M. et al. GDF15, an emerging key player in human aging. *Ageing Res. Rev.* **75**, 101569 (2022).
67. Bando, Y. et al. Kallikrein 6 secreted by oligodendrocytes regulates the progression of experimental autoimmune encephalomyelitis. *Glia* **66**, 359–378 (2018).
68. Yoon, H. et al. Blocking Kallikrein 6 promotes developmental myelination. *Glia* **70**, 430–450 (2022).
69. Goldhardt, O. et al. Kallikrein-related peptidases 6 and 10 are elevated in cerebrospinal fluid of patients with Alzheimer's disease and associated with CSF-TAU and FDG-PET. *Transl. Neurodegener.* **8**, 25 (2019).
70. Patra, K. et al. Assessment of kallikrein 6 as a cross-sectional and longitudinal biomarker for Alzheimer's disease. *Alzheimers Res. Ther.* **10**, 9 (2018).
71. Hahn, O. et al. Atlas of the aging mouse brain reveals white matter as vulnerable foci. *Cell* **186**, 4117–4133.e22 (2023).

72. Piehl, N. et al. Cerebrospinal fluid immune dysregulation during healthy brain aging and cognitive impairment. *Cell* **185**, 5028–5039 (2022).
73. Fujita, S. et al. Characterization of brain volume changes in aging individuals with normal cognition using serial magnetic resonance imaging. *JAMA Netw. Open* **6**, e2318153 (2023).
74. Xu, M. et al. JAK inhibition alleviates the cellular senescence-associated secretory phenotype and frailty in old age. *Proc. Natl Acad. Sci. USA* **112**, E6301–E6310 (2015).
75. Eldjarn, G. H. et al. Large-scale plasma proteomics comparisons through genetics and disease associations. *Nature* **622**, 348–358 (2023).
76. Sudlow, C. et al. UK Biobank: an open access resource for identifying the causes of a wide range of complex diseases of middle and old age. *PLoS Med.* **12**, e1001779 (2015).
77. Miller, K. L. et al. Multimodal population brain imaging in the UK Biobank prospective epidemiological study. *Nat. Neurosci.* **19**, 1523–1536 (2016).
78. Guan, S., Jiang, R., Meng, C. & Biswal, B. Brain age prediction across the human lifespan using multimodal MRI data. *Geroscience* **46**, 1–20 (2024).
79. Wen, J. et al. The genetic architecture of multimodal human brain age. *Nat. Commun.* **15**, 2604 (2024).
80. Wu, T. et al. clusterProfiler 4.0: a universal enrichment tool for interpreting omics data. *Innovation (Camb.)* **2**, 100141 (2021).
81. Garcia, F. J. et al. Single-cell dissection of the human brain vasculature. *Nature* **603**, 893–899 (2022).
82. Zhu, H. et al. Human PBMC scRNA-seq-based aging clocks reveal ribosome to inflammation balance as a single-cell aging hallmark and super longevity. *Sci. Adv.* **9**, eabq7599 (2023).
83. Morabito, S. et al. Single-nucleus chromatin accessibility and transcriptomic characterization of Alzheimer's disease. *Nat. Genet.* **53**, 1143–1155 (2021).
84. Butler, A., Hoffman, P., Smibert, P., Papalexi, E. & Satija, R. Integrating single-cell transcriptomic data across different conditions, technologies, and species. *Nat. Biotechnol.* **36**, 411–420 (2018).
85. Korsunsky, I. et al. Fast, sensitive and accurate integration of single-cell data with Harmony. *Nat. Methods* **16**, 1289–1296 (2019).
86. Lawlor, D. A., Harbord, R. M., Sterne, J. A. C., Timpson, N. & Davey Smith, G. Mendelian randomization: using genes as instruments for making causal inferences in epidemiology. *Stat. Med.* **27**, 1133–1163 (2008).
87. Ferkingstad, E. et al. Large-scale integration of the plasma proteome with genetics and disease. *Nat. Genet.* **53**, 1712–1721 (2021).
88. Burgess, S., Butterworth, A. & Thompson, S. G. Mendelian randomization analysis with multiple genetic variants using summarized data. *Genet. Epidemiol.* **37**, 658–665 (2013).
89. Hemani, G. et al. The MR-Base platform supports systematic causal inference across the human phenome. *eLife* **7**, e34408 (2018).

Acknowledgements

We thank the UK Biobank participants and team members for providing the demographic, clinical, biological sampling and omics data; authors Garcia et al., Morabito et al. and Zhu et al.

for providing single-cell transcriptomic data; and the deCODE consortium and Y.-P. Wang for providing summary-level GWAS data. This study was supported by grants from the Science and Technology Innovation 2030 Major Projects (no. 2022ZD0211600), National Natural Science Foundation of China (nos. 92249305, 82271471, 82071201 and 82071997), National Key R&D Program of China (no. 2021YFC2500100), Shanghai Municipal Science and Technology Major Project (no. 2018SHZDZX01), Research Start-up Fund of Huashan Hospital (no. 2022QD002), Excellence 2025 Talent Cultivation Program at Fudan University (no. 3030277001), Shanghai Talent Development Funding for The Project (no. 2019074), Shanghai Rising-Star Program (no. 21QA1408700), 111 Project (no. B18015), ZHANGJIANG LAB, Tianqiao and Chrissy Chen Institute, State Key Laboratory of Neurobiology and Frontiers Center for Brain Science of Ministry of Education, Shanghai Center for Brain Science and Brain-Inspired Technology, Fudan University and the Non-profit Central Research Institute Fund of Chinese Academy of Medical Sciences (no. 2020-PT310-01).

Author contributions

W.C. and J.-T.Y. designed the study. W.-S.L. and J.Y. conducted the main analyses and drafted the manuscript. S.-D.C. and Y.Z. contributed to interpretation of results. W.-S.L. and Y.Z. contributed to data collection. J.-F.F., Y.-M.X., W.C. and J.-T.Y. critically revised the manuscript. All authors reviewed and approved the final version of the manuscript, had full access to the data in the study and accept responsibility for its submission for publication.

Competing interests

The authors declare no competing interests.

Additional information

Supplementary information The online version contains supplementary material available at <https://doi.org/10.1038/s43587-024-00753-6>.

Correspondence and requests for materials should be addressed to Yu-Ming Xu, Jin-Tai Yu or Wei Cheng.

Peer review information *Nature Aging* thanks N. Chatterjee, E. Johnson and the other, anonymous, reviewer(s) for their contribution to the peer review of this work.

Reprints and permissions information is available at www.nature.com/reprints.

Publisher's note Springer Nature remains neutral with regard to jurisdictional claims in published maps and institutional affiliations.

Springer Nature or its licensor (e.g. a society or other partner) holds exclusive rights to this article under a publishing agreement with the author(s) or other rightsholder(s); author self-archiving of the accepted manuscript version of this article is solely governed by the terms of such publishing agreement and applicable law.

© The Author(s), under exclusive licence to Springer Nature America, Inc. 2024

Reporting Summary

Nature Portfolio wishes to improve the reproducibility of the work that we publish. This form provides structure for consistency and transparency in reporting. For further information on Nature Portfolio policies, see our [Editorial Policies](#) and the [Editorial Policy Checklist](#).

Statistics

For all statistical analyses, confirm that the following items are present in the figure legend, table legend, main text, or Methods section.

n/a | Confirmed

- The exact sample size (n) for each experimental group/condition, given as a discrete number and unit of measurement
- A statement on whether measurements were taken from distinct samples or whether the same sample was measured repeatedly
- The statistical test(s) used AND whether they are one- or two-sided
Only common tests should be described solely by name; describe more complex techniques in the Methods section.
- A description of all covariates tested
- A description of any assumptions or corrections, such as tests of normality and adjustment for multiple comparisons
- A full description of the statistical parameters including central tendency (e.g. means) or other basic estimates (e.g. regression coefficient) AND variation (e.g. standard deviation) or associated estimates of uncertainty (e.g. confidence intervals)
- For null hypothesis testing, the test statistic (e.g. F , t , r) with confidence intervals, effect sizes, degrees of freedom and P value noted
Give P values as exact values whenever suitable.
- For Bayesian analysis, information on the choice of priors and Markov chain Monte Carlo settings
- For hierarchical and complex designs, identification of the appropriate level for tests and full reporting of outcomes
- Estimates of effect sizes (e.g. Cohen's d , Pearson's r), indicating how they were calculated

Our web collection on [statistics for biologists](#) contains articles on many of the points above.

Software and code

Policy information about [availability of computer code](#)

Data collection No software or code was involved in data collection. The data used is all directly available from the UK Biobank, as described in the paper.

Data analysis This study used open-source software and codes, specifically R (v4.2.0; <https://www.r-project.org/>), glmnet (v4.1-4; <https://github.com/cran/glmnet>), clusterProfiler (v4.7.1.003; <https://github.com/YuLab-SMU/clusterProfiler>), Seurat (v4.1.4; <https://satijalab.org/seurat>), harmony (v0.1.0; <https://github.com/immunogenomics/harmony>), TwoSampleMR (v0.5.6; <https://github.com/MRCIEU/TwoSampleMR>), DEswan (v0.0.0.9001; <https://github.com/lehallib/DEswan>), and ggpubr (v0.6.0; <https://github.com/cran/ggpubr>).

For manuscripts utilizing custom algorithms or software that are central to the research but not yet described in published literature, software must be made available to editors and reviewers. We strongly encourage code deposition in a community repository (e.g. GitHub). See the Nature Portfolio [guidelines for submitting code & software](#) for further information.

Data

Policy information about [availability of data](#)

All manuscripts must include a [data availability statement](#). This statement should provide the following information, where applicable:

- Accession codes, unique identifiers, or web links for publicly available datasets
- A description of any restrictions on data availability
- For clinical datasets or third party data, please ensure that the statement adheres to our [policy](#)

The data used in our study were available from the UK Biobank with restrictions applied. The data used in this study were available in the UK Biobank under

application number 19542, and access to the UK Biobank data can be requested through a standard protocol via the website: <https://www.ukbiobank.ac.uk/register-apply/>. The single-cell transcriptomic data were acquired from GEO database (<https://www.ncbi.nlm.nih.gov/geo/>) with the accession number: GSE173731, GSE174367, and GSE213516.

Research involving human participants, their data, or biological material

Policy information about studies with [human participants or human data](#). See also policy information about [sex, gender \(identity/presentation\), and sexual orientation](#) and [race, ethnicity and racism](#).

Reporting on sex and gender	We took sex into considerations in our study and our findings could apply to both male and female. Sex in the UK Biobank was determined based on self-reporting data via questionnaire, and all included participants gave written informed consent for sharing of individual-level data.
Reporting on race, ethnicity, or other socially relevant groupings	Ethnic background (Field ID 21000) was used to define ethnic background in this study.
Population characteristics	We included participants with both multimodal brain imaging data and plasma proteomics data (n = 4,696). The participants had a mean age of 63.16 years and comprised 53.6% females and 97.1% white ethnicities.
Recruitment	The participants included in the present study were from the UK Biobank, a large-scale prospective cohort with more than 500,000 community dwellers from 22 assessment centers throughout the United Kingdom between 2006 and 2010. The demographic characteristics, biological samples, and physical measurements of each participant were obtained at the recruitment, and all participants were registered with the UK National Health Service.
Ethics oversight	The UK Biobank obtained ethics approval from the North West Multicenter Research Ethical Committee and each participant has given written informed consent at the baseline.

Note that full information on the approval of the study protocol must also be provided in the manuscript.

Field-specific reporting

Please select the one below that is the best fit for your research. If you are not sure, read the appropriate sections before making your selection.

Life sciences Behavioural & social sciences Ecological, evolutionary & environmental sciences

For a reference copy of the document with all sections, see [nature.com/documents/nr-reporting-summary-flat.pdf](https://www.nature.com/documents/nr-reporting-summary-flat.pdf)

Life sciences study design

All studies must disclose on these points even when the disclosure is negative.

Sample size	No statistical methods were used to calculate the sample size. We screened the participants with both multimodal brain imaging data and plasma proteomics data (n = 4,696). The sample size was similar to the study reported in previous publication.
Data exclusions	Participants without multimodal brain imaging data or plasma proteomics data were excluded.
Replication	This was an observational study which did not involve experiments.
Randomization	Samples were randomly arranged by computing program into various batches of omics assay.
Blinding	Each sample was labeled with an numeric ID whose annotation was kept blinded during data collection and analyses.

Reporting for specific materials, systems and methods

We require information from authors about some types of materials, experimental systems and methods used in many studies. Here, indicate whether each material, system or method listed is relevant to your study. If you are not sure if a list item applies to your research, read the appropriate section before selecting a response.

Materials & experimental systems

Methods

- | n/a | Involvement |
|-------------------------------------|--|
| <input checked="" type="checkbox"/> | <input type="checkbox"/> Antibodies |
| <input checked="" type="checkbox"/> | <input type="checkbox"/> Eukaryotic cell lines |
| <input checked="" type="checkbox"/> | <input type="checkbox"/> Palaeontology and archaeology |
| <input checked="" type="checkbox"/> | <input type="checkbox"/> Animals and other organisms |
| <input checked="" type="checkbox"/> | <input type="checkbox"/> Clinical data |
| <input checked="" type="checkbox"/> | <input type="checkbox"/> Dual use research of concern |
| <input checked="" type="checkbox"/> | <input type="checkbox"/> Plants |

- | n/a | Involvement |
|-------------------------------------|---|
| <input checked="" type="checkbox"/> | <input type="checkbox"/> ChIP-seq |
| <input checked="" type="checkbox"/> | <input type="checkbox"/> Flow cytometry |
| <input checked="" type="checkbox"/> | <input type="checkbox"/> MRI-based neuroimaging |

Plants

Seed stocks

Report on the source of all seed stocks or other plant material used. If applicable, state the seed stock centre and catalogue number. If plant specimens were collected from the field, describe the collection location, date and sampling procedures.

Novel plant genotypes

Describe the methods by which all novel plant genotypes were produced. This includes those generated by transgenic approaches, gene editing, chemical/radiation-based mutagenesis and hybridization. For transgenic lines, describe the transformation method, the number of independent lines analyzed and the generation upon which experiments were performed. For gene-edited lines, describe the editor used, the endogenous sequence targeted for editing, the targeting guide RNA sequence (if applicable) and how the editor was applied.

Authentication

Describe any authentication procedures for each seed stock used or novel genotype generated. Describe any experiments used to assess the effect of a mutation and, where applicable, how potential secondary effects (e.g. second site T-DNA insertions, mosaicism, off-target gene editing) were examined.